Energy Science & Engineering

Open Access

MODELING AND ANALYSIS

Electrical and thermal analysis of an intermediate temperature IIR-SOFC system fed by biogas

Giuseppe De Lorenzo & Petronilla Fragiacomo

Department of Mechanical, Energy and Management Engineering, University of Calabria, Arcavacata di Rende, 87036 Cosenza, Italy

Keywords
Biogas, intermediate temperature SOFC, numerical simulation model, SOFC cogenerative energy system

Correspondence
Petronilla Fragiacomo, Department of Mechanical, Energy and Management Engineering, University of Calabria, Arcavacata di Rende, 87036 Cosenza, Italy.
E-mail: petronilla.fragiacomo@unical.it

Funding Information
Italian Ministry of Education, University and Research (MIUR).

Received: 28 October 2017; Revised: 10 January 2018; Accepted: 11 January 2018

doi: 10.1002/ese3.187

Abstract

An Intermediate Temperature Solid Oxide Fuel Cells (IT-SOFC) system fed by not conventional fuels such as biogas can produce electric energy with high conversion efficiency and thermal energy. Inside the energy system, the methane in the biogas is mixed with steam, and then it is converted into carbon monoxide, hydrogen and carbon dioxide through steam reforming and water gas shift chemical reactions in an indirect internal reformer (IIR) mostly and in the SOFC anode minimally. The chemical energy of the electro-oxidation of hydrogen and carbon monoxide produced is directly converted into electric energy in the fuel cell anode. A part of the anode exhaust gas can be recirculated at the IIR inlet and the percentage of this recirculated anode exhaust gas together to the fuel utilization factor influence the performances (electric and thermal powers and efficiencies, primary energy saving and first law efficiency) of the SOFC system in a cogenerative arrangement. Through the simulation model of an IT-SOFC system fed by biogas in cogenerative arrangement, which was formulated ad hoc and implemented in a Matlab environment, the influence of the above-mentioned variables on the IT-SOFC system performances was evaluated. The verification of carbon formation at the anode was made.

Introduction

The fuel cells are well placed in the panorama of sustainable energy options owing to some of their important characteristics, such as low environmental impact, in terms of both polluting gases emissions and noise pollution, and the high-energy conversion efficiency.

Among the different fuel cells according to the type of electrolyte and the operating temperature, the high temperature fuel cells (Solid Oxide Fuel Cells [SOFCs], and Molten Carbonate Fuel Cells [MCFCs]) obtain the highest performance values in terms of energy conversion efficiency [1, 2], power density output, stability, useful life, and versatility with regard to the use of fuels. Furthermore, the use of fuels derived from a renewable source, which can feed the SOFC, is particularly interesting. Compared to conventional technologies SOFCs are able to convert various fuels, such as biogas [3–5] or syngas [6–8] deriving from biomasses, into electric energy distributed where it can be used with high efficiency. In addition, Solid Oxide Cell can produce alternatively electric energy (Fuel Cell mode) and hydrogen (Electrolytic Cell mode) [9].

This type of fuel cell has the peculiarity of generating thermal energy, which can be used for cogeneration purposes. Advances in the chemistry and processing of materials are enabling a reduction in the operating temperature of SOFCs in the so-called intermediate temperature region (IT) between 500 and 750°C [10, 11].

The use of new materials, which work best at intermediate temperature, involves a series of advantages, such as: minor sealing problems, smaller number for Balance of Plant components, simplified thermal management, faster phases of startup and shutdown, and the achievement of a higher thermo-mechanical stability of the fuel cell and a reduced degradation of both the fuel cell and the components of the system that contains it.

In recent years there have been a number of theoretical and experimental studies of IT-SOFC energy systems fed by biofuels [12]. The risk associated with the direct use of biofuel (e.g. biogas, bio-alcohols, biodiesel, etc.), which

generally contain a significant level of contaminants, is extremely high [13], although the SOFC intermediate operating temperature can be useful to achieve an internal reforming of organic fuels.

Commercial SOFCs fed by biogas with Ni-YSZ anode and YSZ electrolyte are subject to an irreversible degradation caused mainly by carbon deposit and by sulfur poisoning [14, 15]. These drawbacks can be solved by adding a purification step for biogas [16] and a chemical process to produce a clean syngas from biogas through steam reforming (SR), partial oxidation, autothermal reforming (ATR) or dry reforming (DR) [17–19].

The addition of a considerable amount of steam (steam to carbon ratio equal to or greater than 2) may avert the carbon, promoting the SR of the fuel [20], which may take place either externally to the fuel cell in a dedicated reformer, which is far from the fuel cell with an external mode (ER), or is coupled to the fuel cell with an internal indirect mode (IIR) or internally to the fuel cell with a direct internal mode (DIR). The required heat for reforming can be obtained through the combustion of a part of fuel in a catalytic burner realizing an autothermal reformer.

In the numerical modeling field of SOFC systems fed by biogas, there are some articles in the literature [21–25]. In all these articles [21–26] SOFCs operate at high temperature. In some of these articles the performance of SOFC systems with steam and/or dry reformer reactors external to the anode with ER mode [21, 24] and of an SOFC-gas turbine system with a steam and DR chemical processes inside the SOFC anode [23] were evaluated. In [25] a 2D steady-state mathematical model of a tubular solid oxide fuel cell with indirect internal reforming (IIRSOFC) has been developed to examine the chemical and electrochemical processes and the effect of different operating parameters on the cell performance.

In this article, the conversion of suitable purified biogas into a H_2-rich gas mostly takes place outside the SOFC anode in a reformer with IIR mode through the SR chemical process favored by the heat generated by SOFC, that operates at intermediate temperature. Later the same conversion is completed inside the SOFC anode with DIR mode by the same SR chemical process that is favored by both the SOFC intermediate temperature and the direct H_2 and CO consumptions inside the same anode. In an SOFC a part of the anode exhaust gas, consisting mainly of steam and carbon dioxide (CO_2), can be recirculated at the anode inlet and the fraction of the recirculated anode exhaust gas influences the electric power produced by the fuel cell and the thermal power in output of the fuel cell in an energy system that includes it [2, 26–28].

In this article, a part of the anode exhaust gas, containing mainly steam and CO_2, is recirculated to the reformer inlet, to reduce the amount of steam necessary to the reformer, which has to be produced externally to the SOFC, for increasing the thermal power produced by the IT-SOFC system in a cogenerative arrangement.

This configuration was chosen because it allows one to preserve the SOFC as much as possible and to increase the useful life of the SOFC and because the heat necessary to the SR of biogas is totally supplied by SOFC.

The fuel utilization factor and the recirculation factor of anode exhaust gas affect the IT-SOFC system performances, in terms of electric and thermal powers produced, of the electrical, thermal, and first law efficiencies and the primary energy saving (PES).

The influence of the above-mentioned variables on system performance was evaluated through the simulation model of an IT-SOFC system, fed by biogas and in cogenerative arrangement, which was formulated and implemented in a Matlab environment. The IT-SOFC system simulation model considers the chemical reactions of SR and water gas shift inside the reformer and the same chemical reactions with the electrochemical anodic reaction of CO and H_2 consumptions at the IT-SOFC anode.

Through numerical simulations the trends of the mass flow rates, temperatures and compositions of the working fluids in the IT-SOFC system analyzed were evaluated as a function of some of its characteristic parameters, such as the fuel utilization factor and the recirculation fraction of the anode exhaust gas at the reformer inlet for an equimolar biogas composition.

The IT-SOFC system performances, in terms of electrical and thermal powers produced, the electrical, thermal and first law efficiencies and the PESs, were evaluated as a function of the same above-mentioned characteristic parameters and the regions of variation in these characteristic parameters, in which the IT-SOFC system obtains the highest values of the performances, were identified.

Finally, a verification on formation of carbon, which may be produced inside the anode, was conducted.

Numerical Simulation Model

The simplified lay-out of the IT-SOFC system in cogenerative arrangement considered is shown in Figure 1. It comprises an SOFC, which supplies a direct current user (U), an indirect internal reformer (IIR), a burner (B), and a heat exchanger (HE).

Chemical reactions

In IIR, which is fed by a gas mixture of biogas and steam and by a part of the anode exhaust gas, SR (1.1) and Water Gas Shift (WGS) (1.2) chemical reactions take place:

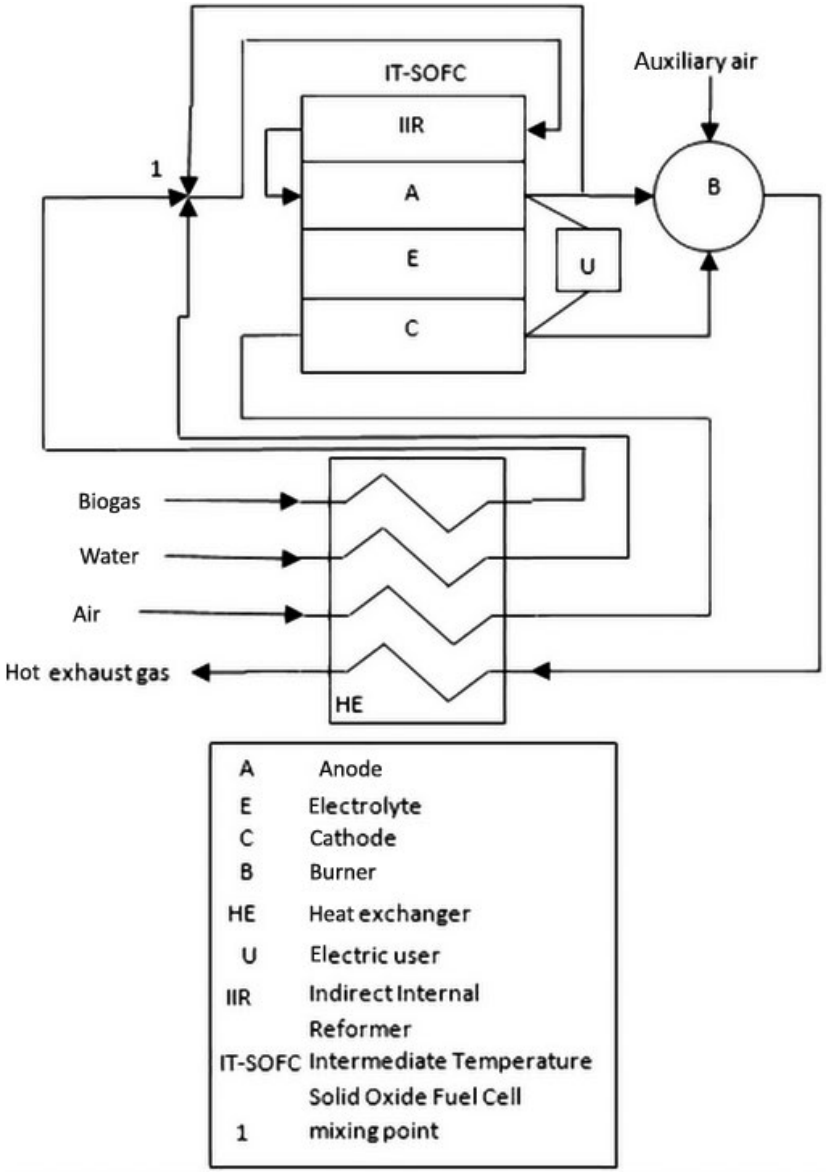

Figure 1. IT-SOFC system fed by biogas in cogenerative arrangement.

$$CH_4 + H_2O \leftrightarrow CO + 3H_2, \quad (1.1)$$

$$CO + H_2O \leftrightarrow H_2 + CO_2. \quad (1.2)$$

The IIR operating temperature is equal to the operating one of the SOFC, which works at intermediate temperature (700°C). In the presence of steam and at intermediate temperature, the SR chemical reaction is much more favored than the DR chemical reaction, which can be neglected. The reformer exhaust gas consists mainly of CO, H_2, and CO_2 and of a small CH_4 percentage.

The electrochemical reactions (2.1) and (2.2) and chemical reactions (1.1) and (1.2), albeit minimally, take place at the SOFC anode, which is fed by the reformer exhaust gas:

$$H_2 + O^{2-} \rightarrow H_2O + 2e^-, \quad (2.1)$$

$$CO + O^{2-} \rightarrow CO_2 + 2e^-. \quad (2.2)$$

The conversion of biogas into an H_2-rich gas occurs mainly in the reformer with IIR mode by chemical reactions (1.1) and (1.2) total favored by the SOFC intermediate operating temperature (700°C). Later, the same conversion completed in the SOFC anode with DIR mode by the same chemical reactions altogether favored by both the SOFC intermediate operating temperature and the

direct H_2 and CO consumptions at the anode through the electrochemical reactions (2.1) and (2.2).

The electrochemical reaction (3) takes place at the cathode:

$$\frac{1}{2}O_2 + 2e^- \rightarrow O^{2-}. \quad (3)$$

Electric energy is produced by the overall SOFC chemical reactions (4) and (5):

$$H_2 + \frac{1}{2}O_2 \rightarrow H_2O, \quad (4)$$

$$CO + \frac{1}{2}O_2 \rightarrow CO_2. \quad (5)$$

A part of CO in reformed feeding gas is used by SOFC, to produce electric energy directly through the electrochemical reactions (2.2) and (3).

IT-SOFC system

The feeding biogas, before entering the reformer, is mixed with the recirculated anode exhaust gas and with steam (mixing point 1).

The gas mixture of biogas, steam and recirculated anode exhaust gas enters the reformer at the temperature $T_{b-S-raeg,in,iir}$, such that reformer catalytic layer works properly, and exits transformed from the reformer at the SOFC average operating temperature T_c.

The reformed gas and air enter in the anode and in the cathode, respectively, at the SOFC average operating temperature, T_c, neglecting the thermal energy loss in the stretch linking IIR and anode, and at the temperature $T_{air,in,ca}$, such that SOFC electrolyte works properly. At the SOFC anode electrochemical reactions (2.1) and (2.2) and the chemical reactions (1.1) and (1.2) encourage the further and almost complete conversion of CH_4 into H_2. The anode and cathode exhaust temperatures are equal to the SOFC average operating temperature, T_c.

A part of the anode exhaust gas is recirculated at the reformer inlet, until the mass flow rate of gas at the SOFC anode inlet reaches the maximum value imposed.

In the HE biogas and water preheat from their feeding temperatures, T_{bio} and T_{H_2O}, up to the mixing temperature with the recirculated anode exhaust gas, T_1, and the air preheat from its feeding temperature, T_{air}, up to its inlet temperature into the SOFC cathode, $T_{air,in,ca}$, thanks to the thermal energy supplied to it by burner B exhaust gas.

The cathode inlet air guarantees the thermal equilibrium of the IIR-SOFC group and is always in excess of that strictly necessary for the functioning of the SOFC.

In the combustor B the non-recirculated anode exhaust gas, which is high-temperature gas with combustible gases (CO and H_2), completely oxidizes thanks to the cathode exhaust gas, which contains oxygen (O_2). The auxiliary air enters the combustor, only in the case in which the cathode exhaust gas is not sufficient to ensure a complete oxidation of the non-recirculated anode exhaust gas at the IIR inlet, and in a quantity strictly necessary to ensure the full oxidation of the same gas.

The burned gas leaves the combustor B at the oxidation temperature, $T_{gas,out,B}$ and the HE at the temperature $T_{gas,out,HE}$.

In the simulation model, the current collectors and the fuel cell gas distributors are considered equipotential surfaces and the amount of carbon that can be formed in the anode is calculated at chemical equilibrium condition.

Indirect internal reformer

The chemical equilibrium inside the internal indirect reformer (IIR) is governed by the equations (6.1) and (6.2):

$$K_{sr} = \frac{\left(\begin{array}{c} (F_{CO,in,iir} + F_{CH_4,sr} - F_{CO,wgs,iir}) \cdot p_{iir}^2 \cdot \\ \cdot (3 \cdot F_{CH_4,sr,iir} + F_{H_2,in,iir} + F_{CO,wgs.iir})^3 \end{array} \right)}{\left(\begin{array}{c} (F_{CH_4,in,iir} - F_{CH_4,sr,iir}) \cdot (F_{H_2O,in,iir} - F_{CH_4,sr,iir} - F_{CO,wgs,iir}) \cdot \\ \cdot \left(\begin{array}{c} F_{CH_4,in,iir} + F_{H_2O,in,iir} + F_{CO_2,in,iir} + F_{H_2,in,iir} + \\ + F_{CO,in,iir} + F_{N_2,in,iir} + 2 \cdot F_{CH_4,sr,iir} \end{array} \right)^2 \end{array} \right)}, \quad (6.1)$$

$$K_{wgs} = \frac{\left(\begin{array}{c} (F_{CO_2,in,iir} + F_{CO,wgs,iir}) \cdot \\ \cdot (3 \cdot F_{CH_4,sr,iir} + F_{H_2,in,iir} + F_{CO,wgs,iir}) \end{array} \right)}{\left(\begin{array}{c} (F_{CO,in,iir} + F_{CH_4,sr,iir} - F_{CO,wgs,iir}) \cdot \\ \cdot (F_{H_2O,in,iir} - F_{CH_4,sr,iir} - F_{CO,wgs,iir}) \end{array} \right)}, \quad (6.2)$$

where K_{sr} and K_{wgs} are the equilibrium constants of chemical reactions (1.1) and (1.2), calculated at the IIR average operating temperature, which is assumed to be equal to the average SOFC operating temperature of the, T_c; $F_{CO,wgs,iir}$ and $F_{CH_4,sr,iir}$ are, respectively, the CO and CH_4 molar flows converted into H_2 and CO inside the IIR through chemical reactions (1.1) and (1.2).

The equations (6.1) and (6.2) govern the equilibrium of the chemical reactions (1.1) and (1.2).

The molar flows of the IIR exhaust gas constituents (H_2O, CO, CO_2, H_2, N_2, CH_4) are calculated using equations (6.3):

$$\begin{array}{c} F_{i,out,iir} - F_{i,in,iir} = \sum_{j=1.1,1.2} (\nu_{i,j} \cdot F_j) \\ \text{with } F_{1.1} = F_{CH_4,sr,iir},\ F_{1.2} = F_{CO,wgs,iir} \\ \text{and } i = CH_4, H_2O, CO, CO_2, H_2, N_2 \end{array} \quad (6.3)$$

where $\nu_{i,j}$ is the stoichiometric coefficient of the ith constituent in the chemical reaction jth, which is positive or

negative in cases in which the same constituent is, respectively, a product or a reactant in the chemical reaction jth.

Fuel cell

Main equations inside the anode are (7.1), (7.2), (7.3), and (7.4):

$$K_{sr}=\frac{\left(\begin{array}{c}(F_{CO,in,a}+F_{CH_4,sr,a}-F_{CO,b}-F_{CO,wgs,a})\cdot p_c^2\cdot\\ \cdot(3\cdot F_{CH_4,sr,a}+F_{H_2,in,a}-F_{H_2,b}+F_{CO,wgs,a})^3\end{array}\right)}{\left(\begin{array}{c}(F_{CH_4,in,a}-F_{CH_4,sr,a})\left(F_{H_2O,in,a}-F_{CH_4,sr,a}+F_{H_2,b}-F_{CO,wgs,a}\right)\cdot\\ \cdot\left(\begin{array}{c}F_{CH_4,in,a}+F_{H_2O,in,a}+F_{CO_2,in,a}+F_{H_2,in,a}+\\ +F_{CO,in,a}+F_{N_2,in,a}+2\cdot F_{CH_4,sr,a}\end{array}\right)^2\end{array}\right)}, \tag{7.1}$$

$$K_{wgs}=\frac{\left(\begin{array}{c}\left(F_{CO_2,in,a}+F_{CO,b}+F_{CO,wgs,a}\right)\cdot\\ \cdot(3\cdot F_{CH_4,sr,a}+F_{H_2,in,a}-F_{H_2,b}+F_{CO,wgs,a})\end{array}\right)}{\left(\begin{array}{c}(F_{CO,in,a}+F_{CH_4,sr,a}-F_{CO,b}-F_{CO,wgs,a})\cdot\\ \cdot(F_{H_2O,in,a}-F_{CH_4,sr,a}+F_{H_2,b}-F_{CO,wgs,a})\end{array}\right)}, \tag{7.2}$$

$$\frac{F_{CO,b}}{F_{H_2,b}}=q, \tag{7.3}$$

$$F_{CO,b}+F_{H_2,b}=\frac{j_c A_c}{2\,\mathrm{Fa}}, \tag{7.4}$$

where K_{sr} and K_{wgs} are the equilibrium constants of chemical reactions (1.1) and (1.2), calculated at the average SOFC operating temperature, T_c; $F_{CO,wgs,a}$ and $F_{CH_4,sr,a}$ are the molar flows of CO and CH_4, which are, respectively, converted into H_2 and CO at the anode by chemical reactions (1.1) and (1.2); $F_{CO,b}$ and $F_{H_2,b}$ are the molar flows of CO and H_2 consumed by electrochemical anodic reactions (2.1) and (2.2).

Equations (7.1) and (7.2) govern the equilibrium of the SR and WGS chemical reactions, equation (7.3) defines the parameter q, which represents the ratio of the CO and H_2 molar flows consumed by the electrochemical anodic reactions (2.1) and (2.2), $F_{CO,b}$ and $F_{H_2,b}$, whereas equation (7.4) governs the electrochemical CO and H_2 consumption at the anode.

The parameter q was measured experimentally by Matsuzaki et al. [29] for an H_2-CO-CO_2-H_2O system at the interface between the Ni-YSZ cermet electrode and YSZ electrolyte for two values of the temperature T_c: 1023 and 1273 K.

The parameter q was evaluated by linear extrapolation at the fuel cell operating temperature investigated. The molar flows of the anode exhaust gas constituents (H_2O, CO, CO_2, H_2, N_2, CH_4), $F_{i,out,a}$, are calculated through equations (7.5):

$$\begin{array}{c}F_{i,out,a}-F_{i,in,a}=\sum_{j=1.1,1.2,2.1,2.2}(\nu_{i,j}\cdot F_j)\\ \text{with}\begin{cases}F_{1.1}=F_{CH_4,sr,a}, F_{1.2}=F_{CO,wgs,a},\\ F_{2.1}=F_{H_2,b}, F_{2.2}=F_{CO,b}\end{cases}\\ \text{and } i=\mathrm{CH_4, H_2O, CO, CO_2, H_2, N_2}\end{array} \tag{7.5}$$

The molar flows of H_2O, CO, CO_2, H_2, N_2, CH_4 recirculated at the IIR inlet, $F_{i,rec,iir}$, are calculated using equation (8):

$$F_{i,rec,iir}=f_{rec}\cdot F_{i,out,a};\ i=\mathrm{H_2O, CO, CO_2, H_2, N_2, CH_4}, \tag{8}$$

where f_{rec} is the recirculation factor.

At the cathode, the fundamental equation is equation (9.1):

$$F_{O_2,b}=0.5\cdot\frac{j_c A_c}{2\,\mathrm{Fa}}. \tag{9.1}$$

If technical air, which is composed only of O_2 and N_2, is considered as cathode feeding gas, the molar flows of O_2 and N_2 at the cathode outlet, $F_{O_2,out,ca}$ and $F_{N_2,out,ca}$, are calculated using equations (9.2):

$$\begin{array}{l}F_{i,out,ca}-F_{i,in,ca}=\nu_{i,3}\cdot F_3\\ \text{with } F_3=F_{O_2,b} \text{ and } i=\mathrm{O_2, N_2}\end{array} \tag{9.2}$$

Energy Analysis of Cogenerative Plant

When the fuel cell is fed by the indirect internal reformer exhaust gas, which is a gas mixture mainly consisting of CO and H_2, similar to a syngas, the real fuel cell voltage, V_c, is calculated by the equation (10) [2, 30, 31]:

$$\begin{aligned}V_c&=V_{N,H_2/O_2}-\Delta V_{act,a,H_2}-\Delta V_{act,ca,O_2}-R_c\cdot j_c\\ &=V_{N,CO/O_2}-\Delta V_{act,a,CO}-\Delta V_{act,ca,O_2}-R_c\cdot j_c\end{aligned} \tag{10}$$

where $V_{N,H_2/O_2}$ and $V_{N,CO/O_2}$ are the Nernst voltages produced by the chemical reactions (4) and (5), respectively; $\Delta V_{act,a,CO}$, $\Delta V_{act,a,H_2}$ and $\Delta V_{act,ca,O_2}$ are the activation voltage losses in the anode and at the cathode. In this article, the SOFC in cogenerative arrangement is considered to operate in the low to medium current density region, where the concentration voltage losses are expected to be limited [25, 32] in order to extend its working life. Therefore, in equation (10) the concentration voltage losses in the anode and the cathode are neglected.

Activation voltage losses for H_2, $\Delta V_{act,a,H_2}$, are calculated through the equation (11) [2, 30, 31]:

$$\begin{array}{c}j_{H_2,a}=\frac{2.1\cdot10^{11}\cdot\exp\left(\frac{-1.2\cdot10^5}{\mathcal{R}\cdot T_c}\right)\cdot p_{H_2O}^{-0.266}\cdot\mathcal{R}\cdot T_c}{(K_{H_2/O_2}\cdot p_{H_2})^{0.266}\cdot\mathrm{Fa}}\cdot\\ \cdot\left[\exp\left(\frac{2\cdot\mathrm{Fa}\cdot\Delta V_{act,a,H_2}}{\mathcal{R}\cdot T_c}\right)-\exp\left(\frac{-\mathrm{Fa}\cdot\Delta V_{act,a,H_2}}{\mathcal{R}\cdot T_c}\right)\right]\end{array}, \tag{11}$$

where $j_{H_2,a}$ is the current density produced by the electrochemical reaction (2.1); K_{H_2/O_2} is the equilibrium constant of the chemical reaction (4).

The activation voltage losses for O_2, $\Delta V_{act,ca,O_2}$, are calculated using the equation (12) [2, 30, 33]:

$$j_{O_2,ca} = \frac{0.25\cdot 10^{10}\cdot \exp\left(\frac{-1.3\cdot 10^5}{\mathcal{R}\cdot T_c}\right)\cdot p_{O_2}^{-0.5}\cdot \mathcal{R}\cdot T_c}{Fa}\cdot \left[\exp\left(\frac{2\cdot Fa\cdot \Delta V_{act,ca,O_2}}{\mathcal{R}\cdot T_c}\right) - \exp\left(\frac{-2\cdot Fa\cdot \Delta V_{act,ca,O_2}}{\mathcal{R}\cdot T_c}\right)\right], \quad (12)$$

where $j_{O_2,ca}$ is the current density produced by the electrochemical reaction (3); Voltage losses for CO activation, $\Delta V_{act,a,CO}$, are calculated by the equation (13) [2, 30, 33]:

$$j_{CO,a} = \frac{CO\cdot \exp\left(\frac{-1.2\cdot 10^5}{\mathcal{R}\cdot T_c}\right)\cdot p_{CO_2}^{-0.266}\cdot \mathcal{R}\cdot T_c}{(K_{CO/O_2}\cdot \bar{p}_{CO})^{0.266}\cdot Fa}\cdot \left[\exp\left(\frac{2\cdot Fa\cdot \Delta V_{act,a,CO}}{\mathcal{R}\cdot T_c}\right) - \exp\left(\frac{-Fa\cdot \Delta V_{act,a,CO}}{\mathcal{R}\cdot T_c}\right)\right], \quad (13)$$

where $j_{CO,a}$ is the current density produced by the electrochemical reaction (2.2); K_{CO/O_2} is the equilibrium constant of the chemical reaction (5).

The parameter CO is constant and its value is calculated in such a way as the condition expressed by the equation (14) occurs [2]:

$$\frac{F_{CO,b}}{F_{H_2,b}} = \frac{j_{CO,a}}{j_{H_2,a}} = q, \quad (14)$$

therefore its value depends on the value of parameter q.

The current density produced by the fuel cell, j_c, is calculated by equation (15):

$$j_c = j_{H_2,a} + j_{CO,a} = j_{O_2,ca}. \quad (15)$$

The electric power produced by the IT-SOFC system, $P_{el,SS}$, is calculated using equation (16):

$$P_{el,SS} = V_c \cdot j_c \cdot A_c. \quad (16)$$

The IT-SOFC system electrical efficiency, $\eta_{el,SS}$, is calculated through equation (17):

$$\eta_{el,SS} = \frac{P_{el,SS}}{G_{bio}\cdot LHV_{bio}}, \quad (17)$$

where G_{bio} and LHV_{bio} are the mass flows and the low heating value of feeding biogas at the inlet of the IT-SOFC system considered.

The thermal power surplus produced by the fuel cell, $P_{th,c}$, is calculated by equation (18) [26]:

$$\begin{aligned} P_{th,c} &= P_{th,lost,c} + P_{th,wgs,a} - P_{th,sr,a} \\ &= F_{H_2,b}\cdot T_c \cdot \Delta\tilde{S}_{H_2/O_2} + F_{CO,b}\cdot T_c \cdot \Delta\tilde{S}_{CO/O_2} \\ &+ (R_c \cdot j_c + \Delta V_{act,c})\cdot j_c \cdot A_c \\ &+ F_{CO,wgs,a}\cdot \Delta\tilde{H}_{wgs} - F_{CH_4,sr,a}\cdot \Delta\tilde{H}_{sr} \end{aligned} \quad (18)$$

where $P_{th,wgs,a}$ and $P_{th,sr,a}$ are the thermal powers produced and consumed by the WGS and SR chemical reactions in the anode. $P_{th,c}$ must be removed to avoid the fuel cell overheating.

The thermal power needed for preheating the feeding gases of the fuel cell, $P_{th,tot,ph}$, is calculated through an equation formulated by the authors ([2] (eq. 21)).

The thermal power needed for heating the IIR, $P_{th,iir}$, is calculated by equation (19):

$$\begin{aligned} P_{th,iir} &= P_{th,wgs,iir} - P_{th,sr,iir} = \\ & F_{CH_4,sr,iir}\cdot \Delta\tilde{H}_{sr} - F_{CO,wgs,iir}\cdot \Delta\tilde{H}_{wgs} \end{aligned} \quad (19)$$

The fuel cell is in thermal equilibrium condition if equation (20) is verified:

$$P_{th,c} - P_{th,tot,ph} - P_{th,iir} = 0. \quad (20)$$

Equation (20) expresses the equality of the thermal power $P_{th,c}$ and the sum of the thermal powers $P_{th,tot,ph}$ and $P_{th,iir}$.

The burner B thermal balance is expressed by equation (21):

$$\eta_{th,B}\left\{\begin{array}{c} \sum_i^{n_{cs,nraeg}}\left[n_{mol,i}\cdot \tilde{H}_i\left(T_c\right)\right] + \sum_j^{n_{cs,gas,out,ca}}\left[n_{mol,j}\cdot \tilde{H}_j\left(T_c\right)\right] \\ + \sum_h^{n_{cs,aux\ air}}\left[n_{mol,h}\cdot \tilde{H}_h\left(T_{in,aux\ air}\right)\right] \end{array}\right\} = \sum_k^{n_{cs,gas,out,B}}\left[n_{mol,k}\cdot \tilde{H}_k\left(T_{out,gas,B}\right)\right] \quad (21)$$

In equation (21) the two members represent the net thermal energy of the reactants (not-recirculated anode exhaust gas, the cathode exhaust gas, and auxiliary air) and the thermal energy of the combustion products.

The thermal balance of HE is expressed by an equation similar to that given by the authors ([2] (eq. 24)). The latter equation considers that in the HE of the analyzed system biogas, water and air are preheated. In mixing point 1 in Figure 1 the thermal balance equation is the equation (22):

$$\begin{aligned} & G_{bio}\cdot H_{bio}\left(T_{out,bio,HE}\right) + G_{H_2O}\cdot H_{H_2O}\left(T_{out,H_2O,HE}\right) \\ & + G_{raeg}\cdot H_{raeg}\left(T_c\right) = G_{gas,in,iir}\cdot H_{gas,in,iir}\left(T_{gas,in,iir}\right) \end{aligned} \quad (22)$$

The net thermal power produced by the IT-SOFC system, $P_{th,net,SS}$, is calculated through equation (23):

$$P_{th,net,SS} = G_{gas,out,B}\int_{T_{ref}}^{T_{gas,out,HE}} c_{p,gas,out,B}(T)\,dT, \quad (23)$$

where T_{ref} is the reference temperature used to calculate this thermal power.

The IT-SOFC system thermal efficiency, $\eta_{th,SS}$, is calculated using equation (24):

$$\eta_{th,SS} = \frac{P_{th,net,SS}}{G_{bio}\cdot LHV_{bio}}. \quad (24)$$

The IT-SOFC system first law efficiency, $\eta_{I,SS}$, is calculated through equation (25):

$$\eta_{\mathrm{I,SS}} = \frac{P_{\mathrm{th,net,SS}} + P_{\mathrm{el,SS}}}{G_{\mathrm{bio}} \cdot \mathrm{LHV}_{\mathrm{bio}}}. \tag{25}$$

Under current legislation (European Commission Delegated Regulation (EU) 2015/2402 of 12/10/2015) the IT-SOFC system fed by biogas for hot water production for sanitary use is a high efficiency cogeneration unit, if it meets the requirements listed in (26):

$$\mathrm{PES}\,(\%) = \left(1 - \frac{1}{\frac{\eta_{\mathrm{th,SS}}}{\eta_{\mathrm{th,ref}}} + \frac{\eta_{\mathrm{el,SS}}}{\eta_{\mathrm{el,ref}}}}\right) \cdot 100 \geq 10 \qquad \eta_{\mathrm{I,SS}} \geq 0.75 \tag{26}$$

where PES (%) is the PESs percentage of IT-SOFC system in cogenerative arrangement; $\eta_{\mathrm{th,ref}}$, $\eta_{\mathrm{el,ref}}$ are the thermal and electrical reference efficiencies.

For a cogeneration plant fed by biogas from anaerobic digestion and built by 2016, according to the above laws, $\eta_{\mathrm{th,ref}}$ and $\eta_{\mathrm{el,ref}}$ based on the lower heating value and on the ISO standard atmospheric conditions (ambient temperature of 15°C, pressure of 1.013 bar, relative humidity of 60%) are equal, respectively, to 0.8 and 0.42.

Verification of Anodic Carbonation

The well-known chemical reactions of methane cracking, Boudouard and of steam production [26] take place in the anode with the electrochemical reactions (2.1) and (2.2) and the chemical reactions (1.1) and (1.2) and produce carbon. The product carbon might be deposited on the anode, causing the progressive deactivation of the entire fuel cell.

The gases pass through the anode quite quickly and the above chemical reactions could not have time to reach the chemical equilibrium condition. Therefore, the amount of carbon produced by these three chemical reactions in chemical equilibrium condition is definitely larger than or equal to the real amount of carbon produced in the fuel cell anode.

It is possible to refer to the composition of the anode inlet gas or to the composition of the anode exhaust gas or to the average gas composition between the anode inlet and outlet to calculate the amount of carbon produced by the above chemical reactions in equilibrium condition.

The triple chemical equilibrium was modeled numerically through three not-linear equations formulated by the authors ([26] (eq. 24)). In the latter system of equations constants k_7, k_8, and k_9 assume unit value in the chemical equilibrium condition.

Three parameters, which represent the carbon masses produced in chemical equilibrium per unit mass of feeding biogas at the inlet or at the outlet of the anode or average in the same anode condition are defined by equations (27):

$$\begin{aligned} \chi_{\mathrm{C,in,a}} &= \frac{G_{\mathrm{C,in,a}}}{G_{\mathrm{bio}}} \\ \chi_{\mathrm{C,out,a}} &= \frac{G_{\mathrm{C,out,a}}}{G_{\mathrm{bio}}} \\ \chi_{\mathrm{C,m,a}} &= \frac{G_{\mathrm{C,m,a}}}{G_{\mathrm{bio}}} \end{aligned} \tag{27}$$

when parameter χ_{C} is negative or zero it means there is no carbon formation inside the anode in chemical equilibrium condition.

Table 1. Compositions of simulated reformed gases.

	Composition				
Reformed gas n.	H_2	H_2O	CO	CO_2	N_2
1	20	3	20	14	43
2	32	3	45	15	3

Validation of Numerical Simulation Model

The reformed gas at the IIR outlet and at the inlet of the fuel cell contains a very small percentage of CH_4 (below 0.1%), which can be neglected, and its composition is similar to that of a syngas.

In Ref. [33] a planar SOFC operating at a temperature of 800°C was fed by a simulated reformed gas (syngas) at different compositions and by air and it has been electrically tested. The compositions of the simulated reformed gas (syngas) used in experiments [33] and of particular interest in this work are shown in Table 1.

The input data to the SOFC calculation code were chosen to make the comparison between the results of the calculation code and the experimental data found in Ref. [33] as homogeneous as possible.

Figure 2 shows the comparison of the two polarization curves obtained by the calculation code, considering two different types of feeding reformed gas, and the experimental data found in Ref. [33], when the operating SOFC temperature is at 800°C.

The mean absolute percentage error of the voltage, $|(\overline{\mathrm{err}})|(\%)$, is defined in equation (28):

$$|(\overline{\mathrm{err}})|(\%) = \frac{\sum_i^N \left(\frac{|V_{\mathrm{exp,i}} - V_{\mathrm{theo,i}}|}{V_{\mathrm{exp,i}}}\right)}{N} \cdot 100 \tag{28}$$

Figure 2 shows that the percentage average absolute errors are, respectively, at 1.37 and 0.84 for the two reformed gases, therefore, for both the reformed gases there is a good agreement between the theoretical polarization

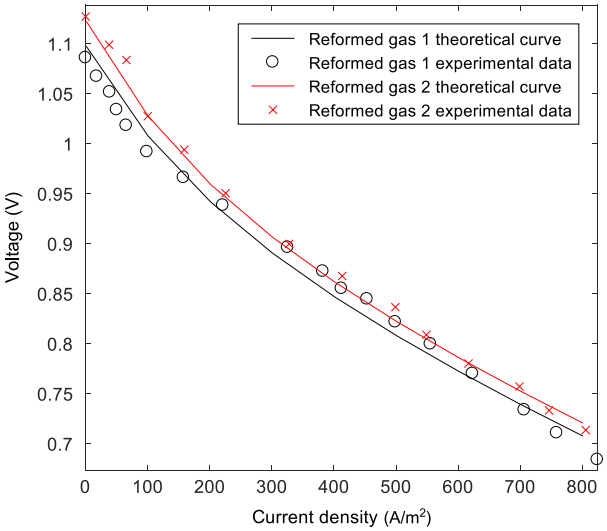

Figure 2. Comparison of the theoretical polarization curves of a fuel cell fed by two different feeding reformed gases (syngases) and the experimental data found in Ref. [33].

curves produced by SOFC calculation code and the experimental data.

Numerical Simulations and Results Analysis

Countless test campaigns were carried out by means of the calculation code implemented in Matlab language. The simplified flowchart of IT-SOFC system calculation code is shown in Figure 3.

The main input data are the variation ranges of the fuel utilization factor and of the anode exhaust gas recirculation factor at the IIR inlet, $\vec{U}_{f,conv}$ and $\vec{f}_{rec}$, the fuel cell active surface, A_c, the biogas and air compositions, $\vec{x}_{bio}$ and $\vec{x}_{air}$, the maximum mass flows of biogas and gas at the system and anode inlets, $G_{max,bio}$ and $G_{max,gas,in,a}$, and the steam to carbon ratio, S/C.

When the input data are loaded, the IT-SOFC system calculation code:

- evaluates the molar flows of all chemical species at the reformer inlet and outlet, $F_{i,in,iir}$ and $F_{i,out,iir}$, and at the anode outlet, $F_{i,out,a}$, by an iterative process;
- verifies whether the anode inlet mass flow, $G_{gas,in,a}$, is greater than the maximum value imposed, $G_{max,gas,in,a}$, and only in this last case recalculates the biogas mass flow at the system inlet, G_{bio}, and the molar flows $F_{i,in,iir}$, $F_{i,out,iir}$, and $F_{i,out,a}$;
- evaluates the molar flows of all the chemical species at the cathode inlet and outlet, $F_{i,in,ca}$ and $F_{i,out,ca}$, the fuel cell voltage, V_c, and the system inlet air mass flow, G_{air}, by another different iterative process;

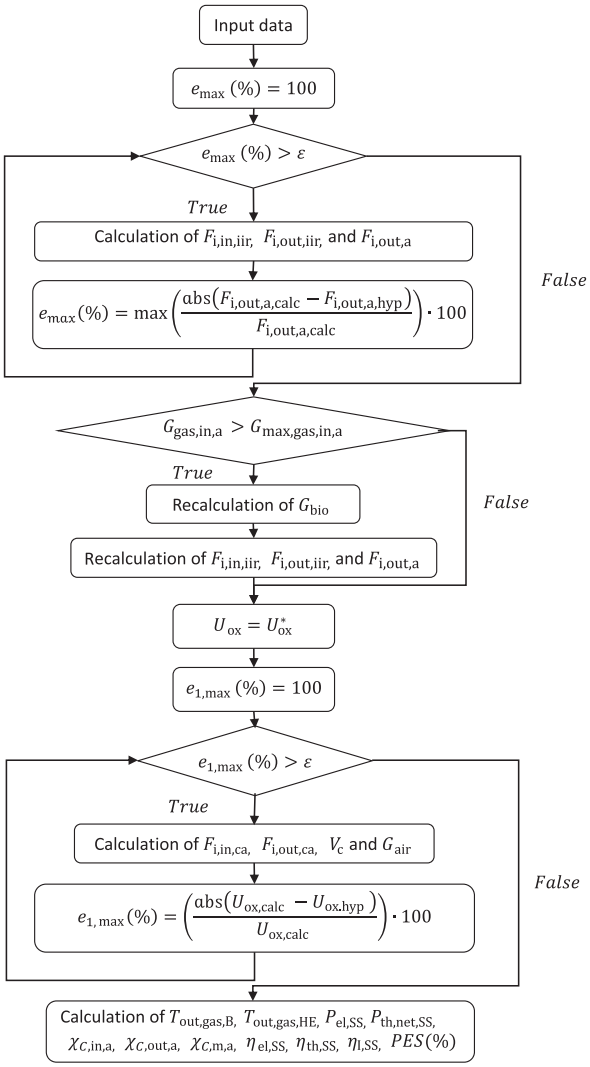

Figure 3. Simplified flow chart of IT-SOFC system calculation code.

- evaluates the burner and HE exhaust gases temperatures, $T_{out,gas,B}$, $T_{out,gas,HE}$, the SOFC system electric and thermal powers, $P_{el,SS}$, $P_{th,net,SS}$, the anode carbonation parameters, $\chi_{C,in,a}$, $\chi_{C,out,a}$, $\chi_{C,m,a}$, and IT-SOFC system electrical, thermal, first law efficiencies, $\eta_{el,SS}$, $\eta_{th,SS}$, and $\eta_{I,SS}$, and PES percentage.

In the most significant test campaign, the results of which are shown in this article, the calculation code was used to simulate the IT-SOFC system fed by an equimolar biogas (50% CH_4 and 50% CO_2) varying the fuel utilization factor and the anode exhaust gas recirculation factor at the IIR inlet. In this test campaign, the main input data of calculation code are given in Table 2.

The maximum mass flow of the anode inlet gas was defined through appropriate numerical simulations. When the recirculation factor, f_{rec}, increases, the mass flow of

Table 2. Input data of the more significant test campaign.

Test campaign	1
Parameter	Value
$U_{f,conv} = \frac{F_{CO,b} + F_{H_2,b}}{4 \cdot F_{CH_4,bio}}$	From 0.5 to 0.65 with increment of 0.01
A_c	0.208 m^2
f_{rec}	From 0 to 0.4 with increment of 0.02
$G_{max,gas,in,a}$	3.625E-5 kg s^{-1}
$G_{max,bio}$	1.618E-5 kg s^{-1}
$\vec{x}_{bio} = [x_{CH_4}, x_{H_2O}, x_{CO}, x_{H_2}, x_{CO_2}, x_{N_2}]$	[0.5, 0, 0, 0, 0.5, 0]
$\vec{x}_{air} = [x_{N_2}, x_{O_2}]$	[0.79, 0.21]
$\frac{S}{C} = \frac{F_{H_2O,in,iir}}{F_{CH_4,bio} + F_{CH_4,rec}}$	2
T_c	973.15 K
$p_{tot,c}$	101,325 Pa
q	0.497
T_{H_2O}	298.15 K
T_{bio}	473.15 K
T_{air}	298.15 K
$T_{aux\ air}$	298.15 K

the mixture gas of biogas and steam at the anode inlet has been suitably reduced, so that the overall mass flow in the anode gas inlet, $G_{gas,in,a}$ does not exceed the maximum set value, $G_{max,gas,in,a}$.

For anodes already developed and at the SOFC operating temperature considered (973.15 K) the value of the parameter q is equal to 0.497. From the analysis of numerous test campaigns the influence of the fuel utilization factor and of the recirculation factor on the main parameters characterizing the IT-SOFC system fed by biogas considered was evaluated. Subsequently, from the analysis of the above described test campaigns the influences of the fuel utilization factor and the anode exhaust gas recirculation factor on the IT-SOFC system performances, in terms of electric and thermal power produced, electrical, thermal, and first law efficiencies and PES, and on the anodic carbonation parameters were evaluated.

Figure 4 shows the trend of the electric power generated by the IT-SOFC system, $P_{el,SS}$, varying the anode exhaust gas recirculation factor at the IIR inlet, f_{rec}, and the conventional fuel utilization factor, $U_{f,conv}$.

When $G_{gas,in,a}$ is equal to $G_{max,gas,in,a}$, f_{rec} assumes the value f^*_{rec}. The f^*_{rec} value decreases, if $U_{f,conv}$ increases, and it is between 0.30 and 0.32.

The increasing of f_{rec} and for each value of $U_{f,conv}$ before $P_{el,SS}$ slowly increases, when f_{rec} is lower than f^*_{rec}, since at constant SOFC operating current density, j_c, operating SOFC voltage, V_c, slowly increases. In the same conditions then $P_{el,SS}$ decreases rapidly, when f_{rec} is greater than f^*_{rec}, since j_c decreases rapidly, despite V_c increases.

For each value of f_{rec} $P_{el,SS}$ always increases when $U_{f,conv}$ increases, since j_c increases despite V_c being reduced. The

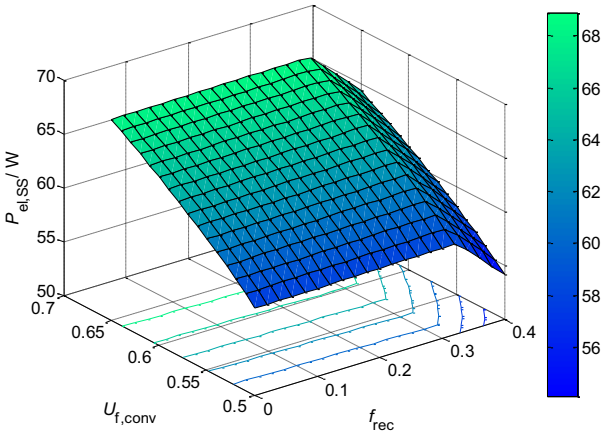

Figure 4. Trend of electric power produced by the IT-SOFC system.

maximum value of electric power is greater than 68 W obtained at the maximum value of $U_{f,conv}$ investigated (0.65) and for f_{rec} equal to f^*_{rec}. In Figure 5 the trend of the net thermal power produced by the IT-SOFC system, $P_{th,net,SS}$, varying f_{rec} and $U_{f,conv}$, is shown.

The increasing of f_{rec} and for each value of $U_{f,conv}$ before $P_{th,net,SS}$ increases rapidly, when f_{rec} is lower than f^*_{rec}, since the mass flow and the temperature of the hot gases at the outlet of the HE, $G_{out,gas,HE}$ and $T_{out,gas,HE}$, increase rapidly. Under the same conditions then $P_{th,net,SS}$ decreases rapidly, when f_{rec} is greater than f^*_{rec}, since $G_{out,gas,HE}$ decreases rapidly, despite $T_{out,gas,HE}$ continues to increase.

When $U_{f,conv}$ increases and for each value of f_{rec} before $P_{th,net,SS}$ increases, since $G_{out,gas,HE}$ increases, despite $T_{out,gas,HE}$ is reduced. When $U_{f,conv}$ increases and for each value of f_{rec} $P_{th,net,SS}$ decreases because $T_{out,gas,HE}$ decreases much faster, despite $G_{out,gas,HE}$ continues to increase.

The maximum value of thermal power is greater than 129 W and this value is reached for $U_{f,conv}$ equal to 0.52 and for f_{rec} equal to f^*_{rec}.

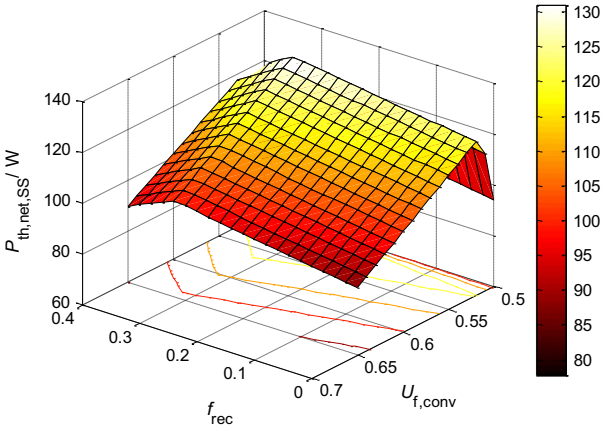

Figure 5. Trend of thermal power produced by the IT-SOFC system.

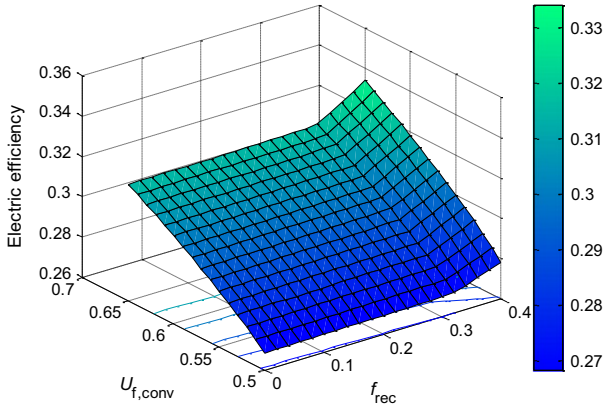

Figure 6. Trend of IT-SOFC system electrical efficiency.

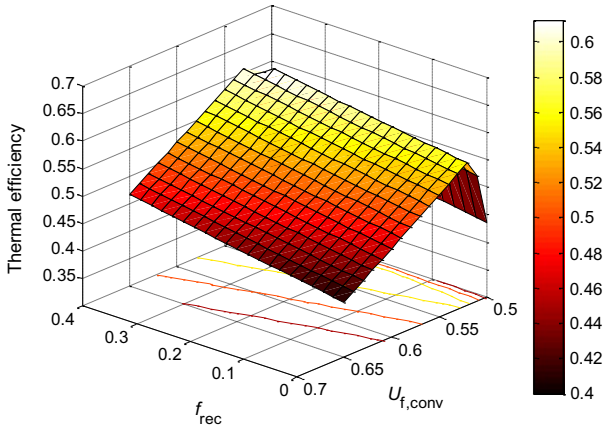

Figure 7. Trend of IT-SOFC system thermal efficiency.

Figures 6 and 7 show the trends of the IT-SOFC system electric and thermal efficiencies, $\eta_{el,SS}$ and $\eta_{th,SS}$, varying f_{rec} and $U_{f,conv}$.

When f_{rec} is lower than f^*_{rec} the mass flow of biogas at the IT-SOFC system inlet, G_{bio}, is constant and equal to the maximum value imposed, $G_{max,bio}$, while when f_{rec} is greater than f^*_{rec}, G_{bio} is progressively reduced to allow the increase in the recirculation gas mass flow at a fixed value of anode inlet gas maximum mass flow.

When f_{rec} is lower than f^*_{rec} the trends of $\eta_{el,SS}$ and $\eta_{th,SS}$ follow the trends of $P_{el,SS}$ and $P_{th,net,SS}$. When f_{rec} is greater than f^*_{rec} the trends of $\eta_{el,SS}$ and $\eta_{th,SS}$ deviate from the trends of $P_{el,SS}$ and $P_{th,net,SS}$ since G_{bio} decreases.

In nominal operating range ($U_{f,conv,min} \le U_{f,conv} \le U_{f,conv,max}$; $0 \le f_{rec} \le f^*_{rec}$) the maximum values of $\eta_{el,SS}$ and $\eta_{th,SS}$ are, respectively, greater than 0.31 for f_{rec} equal to f^*_{rec} and $U_{f,conv}$ equal to $U_{f,conv,max}$ and greater than 0.57 for f_{rec} equal to f^*_{rec} and $U_{f,conv}$ equal to 0.52.

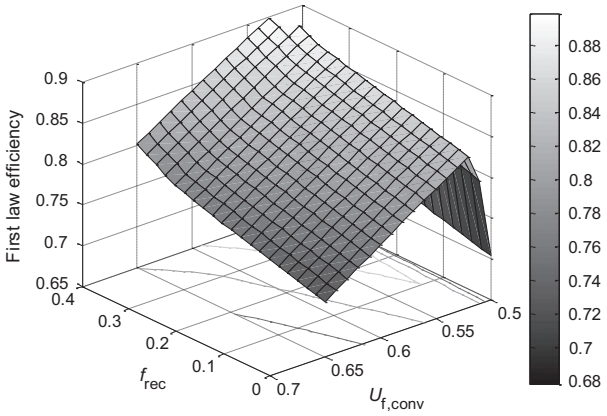

Figure 8. Trend of IT-SOFC system first law efficiency.

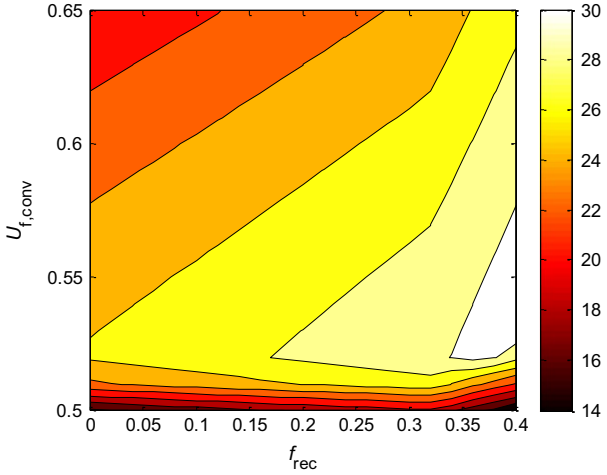

Figure 9. Isolevel curves for the trend of IT-SOFC system primary energy saving.

Figure 8 shows the IT-SOFC system first law efficiency, $\eta_{I,SS}$, varying f_{rec}, and $U_{f,conv}$. Obviously its trend is derived from the trends of $\eta_{el,SS}$ and $\eta_{th,SS}$.

In nominal operating range ($U_{f,conv,min} \le U_{f,conv} \le U_{f,conv,max}$; $0 \le f_{rec} \le f^*_{rec}$) the maximum value of $\eta_{I,SS}$ is greater than 0.88 for f_{rec} equal to f^*_{rec} and $U_{f,conv}$ equal to 0.52.

Figure 9 shows the isolevel curves of PESs, PES, trend, varying the parameters f_{rec} and $U_{f,conv}$.

In nominal operating range ($U_{f,conv,min} \le U_{f,conv} \le U_{f,conv,max}$; $0 \le f_{rec} \le f^*_{rec}$) the maximum value of PES is higher than 30% for f_{rec} equal to f^*_{rec} and $U_{f,conv}$ equal to 0.52.

For f_{rec} equal to f^*_{rec} and $U_{f,conv}$ equal to 0.52 graphs shown up to now show that the IT-SOFC system is certainly considered a cogenerative system, according to current Italian and European legislation, at high efficiency and obtains the best values of PES and $\eta_{I,SS}$. Finally, the

calculation code was used to verify the formation of carbon at the SOFC anode.

Figure 10 shows the trends of the anodic carbonation parameters, $\chi_{C,in,a}$, $\chi_{C,out,a}$, and $\chi_{C,m,a}$, varying f_{rec} and $U_{f,conv}$. As expected, the resulting graphs confirm that there is no carbon formation either at the anode inlet and outlet or on average in the anode, because *S*/*C* ratio is largely precautionary.

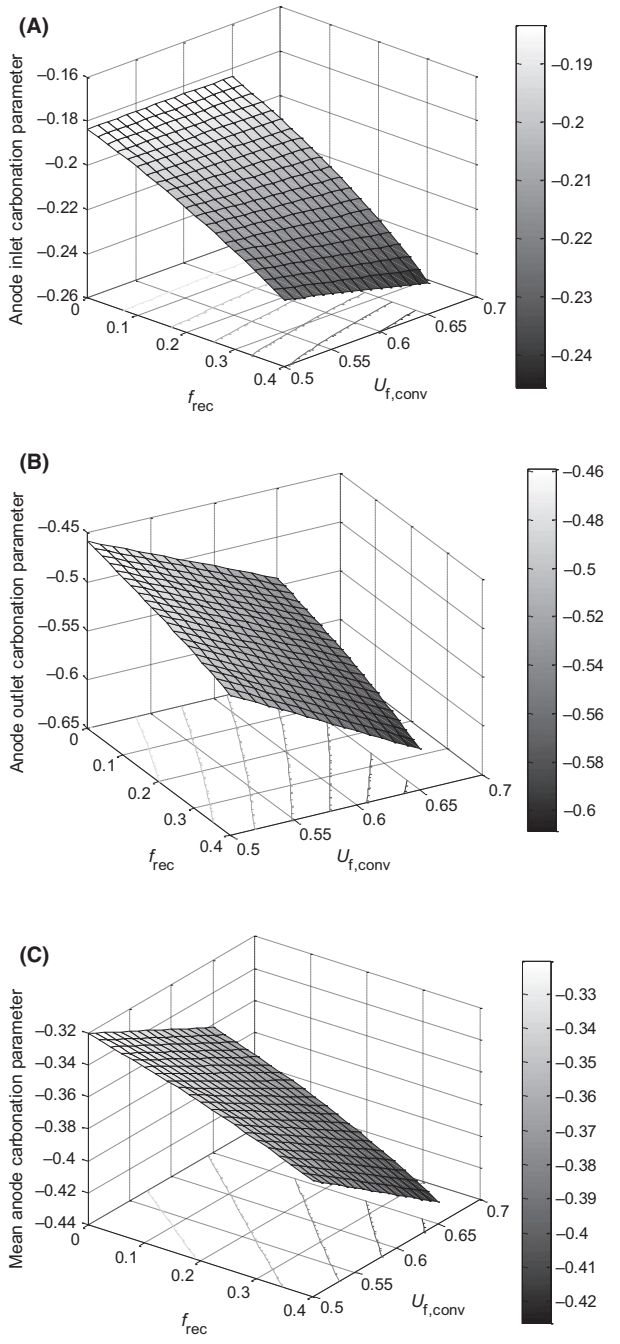

Figure 10. Trends of anodic carbonation parameters: inlet (A), outlet (B), mean (C).

Regarding the carbon formation, the most critical area is the anode inlet section of the fuel cell, since in it the molar flows of CO and H_2 are significant, but in the same section the presence of equally significant CO_2 and steam molar flow rates averts the carbon formation.

Conclusions

The calculation tool set up in this work allows the IT-SOFC energy system fed by biogas in cogenerative arrangement to be described completely.

The energy-cogenerative analysis conducted has permitted output parameters to be obtained such as electrical and thermal powers produced, PES and electrical, thermal and first law efficiencies, as a function of two evaluation parameters, such as the fuel utilization factor and the recirculation fraction of the anode exhaust gas at the internal indirect reformer inlet.

The same calculation tool has made possible the identification of the regions of variation in the above evaluation parameters, in which the IT-SOFC system obtains the highest values of the output parameters chosen.

An analysis of the results showed that the IT-SOFC system is a high-performance cogenerative system, in accordance with Italian and European legislation, and the same system obtains values of electrical, thermal and first law efficiencies greater than 0.31, 0.57, and 0.88 and a PES greater than 30% of the parameters variation in the regions identified.

This calculation tool is very flexible and can also be used to evaluate other output parameters as a function of different evaluation parameters.

Nomenclature

A	= fuel cell surface	m^2
c	= specific heat	$J\ kg^{-1}\ K^{-1}$
err	= percentage error	%
F	= molar flow	$mol\ s^{-1}$
f	= factor	
Fa	= Faraday constant	$C\ mol^{-1}$
G	= mass flow	$kg\ s^{-1}$
H	= enthalpy	$J\ kg^{-1}$
j	= current density	$A\ m^{-2}$
K	= equilibrium constant	
k	= constant	
LHV	= low heating value	$J\ kg^{-1}$
n	= number	
p	= partial pressure	atm
P	= power	W
PES	= Primary Energy Saving	%
q	= ratio between the CO and H_2 molar flows electrochemically consumed	
R	= resistance	$\Omega\ m^2$
$\Re$	= gas constant	$J\ mol^{-1}\ K^{-1}$

S/C	= steam to carbon ratio	
T	= temperature	K
U	= utilization factor	
V	= voltage	V
x	= molar fraction	
ΔH	= enthalpy variation	J mol^{-1} or J kg^{-1}
ΔS	= entropy	J mol^{-1} K^{-1}
ΔV	= voltage loss	V
co	= constant	

Greek letters	
χ	= mass fraction
η	= efficiency
ν	= stoichiometric coefficient

Subscripts	
a	= anode
act	= activation
air	= air
aux	= auxiliary
b	= electrochemically consumed
B	= burner
bio	= biogas
b-s-raeg	= mixture of biogas, steam, and recirculated anode exhaust gases
c	= fuel cell element
C	= carbon
ca	= cathode
CH_4, CO, H_2O, H_2, CO_2, N_2, O_2	= methane, carbon monoxide, water or steam, hydrogen, carbon dioxide, nitrogen, oxygen
CO/O_2	= CO oxidation chemical reaction
conv	= conventional
cs	= chemical species
el	= electric
exp	= experimental
f	= fuel
gas	= gas mixture
H_2/O_2	= H_2 oxidation chemical reaction
HE	= heat exchanger
i, j, h, k	= generic index
Iir	= indirect internal reformer
In	= at the inlet
lost	= lost for chemical irreversibilities, for joule and contact effects and for polarization phenomena
m	= mean
mol	= mole
N	= Nernst
net	= net
nraeg	= not-recirculated anodic exhaust gas
out	= at the outlet
p	= at constant pressure
ph	= preheating
raeg	= recirculated anodic exhaust gas
rec	= anodic recirculation
ref	= reference
sr	= referred to steam reforming chemical reaction
SS	= SOFC system
theo	= theoretical
th	= thermal
tot	= total
tot, max	= total and maximum value
wgs	= referred to water gas shift chemical reaction

Superscripts	
–	= mean value
~	= molar
→	= vector

Acknowledgments

This research activity was developed within the program "PROGRAMMI DI RICERCA SCIENTIFICA DI RILEVANTE INTERESSE NAZIONALE-PRIN- PROGRAMMA DI RICERCA-Anno 2010–2011-prot. 2010- KHLKFC" within the project entitled "Intermediate Temperature Solid Oxide Fuel Cell fed by BIOfuels (BIOITSOFC)" thanks to financial support of Italian Ministry of Education, University and Research (MIUR).

Conflict of Interest

None declared.

References

1. De Lorenzo, G., and P. Fragiacomo. 2012. A methodology for improving the performance of molten carbonate fuel cell/gas turbine hybrid systems. Int. J. Energy Res. 36:96–110.
2. De Lorenzo, G., and P. Fragiacomo. 2012. Electrical and electrical–thermal power plants with molten carbonate fuel cell/gas turbine-integrated systems. Int. J. Energy Res. 36:153–165.
3. Moulod, M., A. Jalali, and R. Asmatulu. 2016. Biogas derived from municipal solid waste to generate electrical power through solid oxide fuel cells. Int. J. Energy Res. 40:2091–2104.
4. Paradis, H., M. Martin Andersson, J. Yuan, and B. Sundén. 2011. Simulation of alternative fuels for potential utilization in solid oxide fuel cells. Int. J. Energy Res. 35:1107–2104.
5. Corigliano, O., G. Florio, and P. Fragiacomo. 2011. A numerical simulation model of high temperature fuel cells fed by biogas. Energy Sources A Rec. Util. Environ. Effects 34:101–110.
6. De Lorenzo, G., and P. Fragiacomo. 2015. Energy analysis of an SOFC system fed by syngas. Energy Convers. Manage. 93:175–186.
7. Murgi, N., G., De Lorenzo, O. Corigliano, F. A. Mirandola, P. Fragiacomo. 2016. Influence of anodic gas

mixture composition on solid oxide fuel cell performance: part 2. Int. J. Heat Technol. 34(Special issue 2):S303–S308.
8. Murgi, N., G. De Lorenzo, O. Corigliano, F. A. Mirandola, P. Fragiacomo. 2016. Influence of anodic gas mixture composition on solid oxide fuel cell performance: part 1. Int. J. Heat Technol. 34(Special issue 2):S309–S314.
9. Milewski, J., M. Wołowicz, and J. Lewandowski. 2017. Comparison of SOE/SOFC system configurations for a peak hydrogen power plant. Int. J. Hydrogen Energy 42:3498–3509.
10. Brett, D. J. L., A. Atkinson, N. P. Brandon, and S. J. Skinner. 2008. Intermediate temperature solid oxide fuel cells. Chem. Soc. Rev. 37:1568–1578.
11. Pikalova, E. Y., A. A. Murashkina, V. I. Maragou, A. K. Demin, V. N. Strekalovsky, and P. E. Tsiakaras. 2011. CeO2 based materials doped with lanthanides for applications in intermediate temperature electrochemical devices. Int. J. Hydrogen Energy 36:6175–6183.
12. Yentekakis, I. V. 2006. Open and closed - circuit study of an intermediate temperature SOFC directly fueled with simulated biogas mixtures. J. Power Sources 160:422–425.
13. Offer, G. J., J. Mermelstein, E. Brightman, and N. P. Brandon. 2009. Thermodynamics and kinetics of the interaction of carbon and sulfur with solid oxide fuel cell anodes. J. Am. Ceram. Soc. 92:763–780.
14. Shiratori, Y., T. Ijichi, T. Oshima, and K. Sasaki. 2010. Internal reforming SOFC running on biogas. Int. J. Hydrogen Energy 35:7905–7912.
15. Vahc, Z. Y., C.-Y. Jung, and S. C. Yi. 2014. Performance degradation of solid oxide fuel cells due to sulfur poisoning of the electrochemical reaction and internal reforming reaction. Int. J. Hydrogen Energy 39:17275–17283.
16. Barelli, L., G. Bidini, N. de Arespacochaga, L. Pérez, and E. Sisani. 2017. Biogas use in high temperature fuel cells: enhancement of KOH-KI activated carbon performance toward H2S removal. Int. J. Hydrogen Energy 42:10341–10353.
17. Ahmed, S., and M. Krumpelt. 2001. Hydrogen from hydrocarbon fuels for fuel cells. Int. J. Hydrogen Energy 26:291–301.
18. Lee, A. L., R. F. Zabransky, and W. J. Huber. 1990. Internal reforming development for solid oxide fuel cells. Ind. Eng. Chem. Res. 29:766–773.
19. Cipitì, F., O. Barbera, N. Briguglio, G. Giacoppo, C. Italiano, and A. Vita. 2016. Design of a biogas steam reforming reactor: a modelling and experimental approach. Int. J. Hydrogen Energy 41:11577–11583.
20. Singhal, S. C. 2000. Advances in solid oxide fuel cell technology. Solid State Ionics 135:305–313.
21. Papurello, D., R. Borchiellini, P. Bareschino, V. Chiodo, S. Freni, A. Lanzini et al. 2014. Performance of a Solid Oxide Fuel Cell short-stack with biogas feeding. Appl. Energy 125:254–263.
22. Dietrich, R. U., J. Oelze, A. Lindermeir, C. Spieker, C. Spitta, and M. Steffen. 2014. Power generation from biogas using SOFC – results for a 1kWe Demonstration Unit. Fuel Cells 14(2):239–250.
23. Wongchanapai, S., H. Iwai, M. Saito, and H. Yoshida. 2013. Performance evaluation of a direct-biogas solid oxide fuel cell-micro gas turbine (SOFC-MGT) hybrid combined heat and power (CHP) system. J. Power Sources 223:9–17.
24. Prodromidis, G. N., and F. A. Coutelieris. 2017. Thermodynamic analysis of biogas fed solid oxide fuel cell power plants. Renew. Energy 108:1–10.
25. Hosseini, S., S. M. Jafarian, and G. Karimi. 2011. Performance analysis of a tubular solid oxide fuel cell with an indirect internal reformer. Int. J. Energy Res. 35:259–270.
26. De Lorenzo, G., O. Corigliano, M. Lo Faro, P. Frontera, P. Antonucci, S. C. Zignani et al. 2016. Thermoelectric characterization of an Intermediate Temperature Solid Oxide Fuel Cell system directly fed by dry biogas. Energy Convers. Manage. 127:90–102.
27. Marsano, F., L. Magistri, and A. F. Massardo. 2004. Ejector performance influence on a solid oxide fuel cell anodic recirculation system. J. Power Sources 129(2):216–228.
28. Zabihian, F., and A. S. Fung. 2013. Performance analysis of hybrid solid oxide fuel cell and gas turbine cycle: application of alternative fuels. Energy Convers. Manage. 76:571–580.
29. Matsuzaki, Y., and I. Yasuda. 2000. Electrochemical oxidation of H_2 and CO in a H_2–H_2O-CO-CO_2 System at the Interface of a Ni-YSZ cermet electrode and YSZ electrolyte. J. Electrochem. Soc. 147:1630–1635.
30. Andersson, M., J. Yuan, and B. Sunden. 2013. SOFC modeling considering hydrogen and carbon monoxide as electrochemical reactants. J. Power Sources 232: 42–54.
31. Beale, S. B. 2005. Chapter 2. Pp. 43–82 *in* B. Sunden, M. Faghri, eds. Transport phenomena in fuel cells. WIT Press, Southampton.
32. Noren, D. A., and M. A. Hoffman. 2005. Clarifying the Butler-Volmer equation and related approximations for calculating activation losses in solid oxide fuel cell models. J. Power Sources 152:175–181.
33. Suwanwarangkul, R., E. Croiset, E. Entechev, S. Charojrochkul, M. D. Pritzer, M. W. Fowler et al. 2006. Experimental and modeling study of solid oxide fuel cell operating with syngas fuel. J. Power Sources 161:308–322.

